

VAPOR PHASE TRANSPORT OF UNEXPLODED ORDNANCE COMPOUNDS
THROUGH SOILSRAGHUNATHAN RAVIKRISHNA,[†] SALLY L. YOST,[‡] CYNTHIA B. PRICE,[§] KALLIAT T. VALSARAJ,^{*†}JAMES M. BRANNON,[§] and PAUL H. MIYARES[§][†]Gordon A. and Mary Cain Department of Chemical Engineering, Louisiana State University, Baton Rouge, Louisiana 70803, USA[‡]DynTel Corporation, 350 Manor Drive, Vicksburg, Mississippi 39180, USA[§]Engineering Research and Development Center, Waterways Experiment Station, U.S. Army Corps of Engineers, 3909 Halls Ferry Road, Vicksburg, Mississippi 39180

(Received 24 April 2001; Accepted 13 March 2002)

Abstract—Unexploded ordnance (UXO) is a source of concern at several U.S. Department of Defense (DOD) sites. Localization of munitions and fate and transport of the explosive compounds from these munitions are a major issue of concern. A set of laboratory experiments were conducted in specially designed flux chambers to measure the evaporative flux of three explosive compounds (2,4-dinitrotoluene, 2,6-dinitrotoluene, and 1,3-dinitrobenzene) from three different soils. The effect of different soil moisture contents, the relative humidity of air contacting the soil surface, and soil temperature on the chemical fluxes were evaluated. A diffusion model was used to describe the chemical transport mechanism in the soil pore air. The soil–air partition constant was treated as a fit parameter in the model because of the uncertainty in the a priori estimation. The model predicts the qualitative trends of the experimental fluxes satisfactorily. Under extremely dry conditions, the flux decreased more rapidly than that predicted by the model. The fluxes from soils at 24°C were higher than those at 14°C, indicating a larger volatilization driving force at the higher temperature.

Keywords—Unexploded ordnance Volatilization Partition constants

INTRODUCTION

Numerous DOD sites are contaminated with explosives, propellants, petroleum hydrocarbons, and heavy metals [1]. The explosive 2,4,6-trinitrotoluene (TNT) and associated compounds form a significant fraction of explosives residues found at some of the DOD sites. Unexploded ordnance at military training installations continue to pose a hazard, either through explosive hazards or contamination of soil and water if the casings are breached.

Extensive documentation exists on the fate and transport of explosives residues from contaminated soils and groundwater under saturated conditions [2]. However, processes controlling the migration of explosives chemical signatures through soil from UXO and other sources under unsaturated conditions are poorly understood. This handicaps the development of chemical sensors and evaluation of existing sensors because the strength of chemical signatures at the detector cannot be predicted. It also hinders development of methods for predicting and evaluating vadose zone transport of explosives.

The fate and transport of explosives in the air-filled pores within soil affects both the potential detection of buried ordnance by chemical sensors and vadose zone transport of explosives residues [2]. The transport characteristics of explosives vapors through soils affect the sensitivity levels that chemical sensors must attain to detect chemical signatures for a given munition depth. Transport characteristics also affect how chemical concentrations will migrate in the vadose zone independent of water phase transport. We have previously de-

veloped experimental and modeling methods for examining the flux of polyaromatic hydrocarbons from sediment and into the air [3–5]. Results have shown that transport from the sediment particles to the air are affected by moisture content, air relative humidity, air velocity, and temperature. When the surface concentrations of the contaminants are depleted, vapor phase transport through the soil or sediment pore spaces controls fluxes from the soil or sediment into the air.

The modeling and experimental methods utilized for examining the fluxes of polyaromatic hydrocarbons can be modified and adapted for examining the transport of explosives from soils under differing conditions of soil moisture, temperature, and relative humidity. These parameters have been shown to control the flux of nonpolar organic compounds from sediment particles into the air [3–5] and provide a basis for the initial evaluation of explosives residues vapor transport.

The objectives of this study were to obtain experimental data, to develop a model of explosives signature transport through soil, and to determine the need for additional process information to adequately describe the transport observed experimentally. Models developed in previous studies [3] that successfully predicted air emissions of polynuclear aromatic hydrocarbons from exposed sediment dredged materials were used as the basis for the explosives signature transport model. Variations of these models were applied to laboratory data measuring the emission of explosives compounds from three different soil types under various environmental conditions.

EXPERIMENTAL

Soil

Two aquifer soils obtained from the Louisiana Army Ammunition Plant (Shreveport, LA, USA) (LAAP-C and LAAP-

* To whom correspondence may be addressed
(valsaraj@che.lsu.edu).

Table 1. Relevant properties of soils and unexploded ordnance (UXO) compounds

Physical characteristics of soils			
Soil property	LAAP-C ^a	LAAP-D ^a	Yokena clay
Percentage sand	77	27	13.75
Percentage silt	11	41	37.54
Percentage clay	12	32	48.75
Textural classification	Sandy loam	Clay loam	Clay
Percentage total organic carbon	0.08	0.20	2.4
Bulk density (g/cm ³)	1.43	0.88	0.86
Relevant properties of UXO compounds			
Property	13-DNB ^b	24-DNT ^c	26-DNT
Molecular weight	168.1	182.1	182.1
Diffusivity in air (cm ² /s) ^d	0.073	0.067	0.067
Henry's constant (-) ^d	3.2×10^{-5}	7.5×10^{-6}	7.5×10^{-6}
Boundary layer mass transfer coefficient; k_a (m/s) ^e	0.00016	0.00015	0.00015
Loading (mg/kg)			
LAAP-C	7.44	10.54	8.37
LAAP-D	9.19	10.95	8.97
Yokena	9.13	9.30	9.36

^a LAAP-C and LAAP-D = two aquifer soils obtained from Louisiana Army Ammunition Plant (Shreveport, LA, USA).

^b DNB = dinitrobenzene.

^c DNT = dinitrotoluene.

^d McGrath [2].

^e Thibodeaux [9].

D) and one surface soil (Yokena clay) from the Mississippi River, USA, floodplain were used to determine fluxes of specified explosive compounds. The soils were chosen so that comparisons could be made of the effects of carbon content and soil characteristics on flux rates. Each soil was air dried, ground, and sieved before storing at room temperature. Physical characteristics of the soils are given in Table 1.

Samples of 800 g of the different soils were spiked with 50 ml of an acetone solution containing 10 ppm of 2,4-dinitrotoluene (2,4-DNT), 2,6-dinitrotoluene (2,6-DNT), and 1,3-dinitrobenzene (1,3-DNB). These compounds are major impurities in TNT but are more volatile and mobile, providing detectable surrogates for the presence of TNT. Table 1 lists the physicochemical properties of the compounds considered in this study, and Table 2 lists the loading of the spiked soils with the three compounds. The spiked soils were placed on a pan in a thin layer under a hood to allow the acetone to evaporate, then tumbled overnight to ensure complete mixing.

Flux chamber studies

We modified and used a test chamber [3] designed by Spencer et al. [6] to measure explosive fluxes from the spiked soils. The two parts of the chamber were constructed of anodized aluminum. The bottom portion held soil at a depth of 2 cm with a surface area of 30 cm². The top portion was designed with channels to provide a 2-mm airspace over the sediment

well to allow uniform airflow across the soil surface. O-rings and threaded fasteners were used to seal the compartments together for an airtight fit.

Laboratory house air entered the chambers through the entrance ports, flowing over the soil surface. Air sampling traps made from stainless-steel tubing containing 0.2 g Tenax® (Tekmar-Dohrmann, Cincinnati, OH, USA) were attached to the exit ports of the chambers to collect explosive compounds released into the airstream.

The experiment was designed to compare volatile emissions under varying air relative humidity (0 and 98%), soil moisture content (5 and 20%), and soil temperature (14 and 24°C). Air humidity was controlled using an in-line bubble trap to add moisture vapor to the passing air. Moisture contents of each soil were determined, and calculated amounts of deionized water were added initially to obtain the desired soil moisture content. A recirculating water bath (model CFF550, Remcor Products Company, Glendale Heights, IL, USA) was set to maintain a constant 14°C for the low temperature experiment, while room temperature conditions were used for the experiment at 24°C.

Air sampling traps were connected to the exit ports of the chambers. Humid airflow was established at the desired flow rate of 20 ml/min and passed over the soils for a 21-d period. The humid air was then switched to dry air for another 21-d period. Air samples were taken at 24, 72, 168, 336, and 504 h during the sampling period by removing the Tenax trap after the desired interval and replacing with a fresh tube for the duration of the next sampling period. The traps were analyzed for the mass of contaminant trapped (Δm). Knowing the duration of sampling (Δt) and the soil-air interface area of the chamber (A_c), the flux rates were determined from $N_A = (\Delta m/A_c \Delta t)$.

Equilibrium adsorption testing

Equilibrium adsorption testing was conducted with LAAP-C, LAAP-D, and Yokena clay. This test was conducted with a 1:4 ratio of soil to water (4 g soil to 16 ml water) with five

Table 2. Initial loading of soils with the three unexploded ordnance (UXO) compounds^a

Soil	Loading (mg/kg)		
	13-DNB	24-DNT	26-DNT
LAAP-C	7.4	10.5	8.4
LAAP-D	9.2	11.0	9.0
Yokena clay	9.1	9.3	9.4

^a Refer to Table 1 for definitions of abbreviations.

Table 3. Soil–water adsorption coefficients (K_{sw} , L/kg) for 2,4-DNT, 2,6-DNT, and 1,3-DNB in three soils^a

Soil	Compound	K_{sw}	r^2
LAAP-C (aquifer soil)	2,4-DNT ^b	0.67	0.85
LAAP-D (aquifer soil)	2,4-DNT	1.67	0.75
Yokena clay	2,4-DNT	12.5	0.95
LAAP-C (aquifer soil)	2,6-DNT	0.96	0.96
LAAP-D (aquifer soil)	2,6-DNT	1.83	0.88
Yokena clay	2,6-DNT	5.96	0.99
LAAP-C (aquifer soil)	1,3-DNB ^b	0.32	0.59
LAAP-D (aquifer soil)	1,3-DNB ^b	No significant adsorption	
Yokena clay	1,3-DNB	17.7	0.95

^a Refer to Table 1 for definitions of abbreviations. r^2 = regression coefficient.

^b Data from Pennington et al. [14].

different concentrations (10, 7.5, 5, 2.5, and 1 $\mu\text{g/ml}$) of contaminant. The LAAP-C test was spiked with 2,6-DNT, the LAAP-D test was spiked with 2,6-DNT and 2,4-DNT in separate runs, while the Yokena clay was spiked with a mixture of contaminants (TNT, 2,4-DNT, 1,3,5-TNB, 1,3-DNB, and 2,6-DNT). Samples were then placed on a reciprocating shaker at 280 excursions/min for 24 h. At the end of the 24 h, the samples were centrifuged at 7,000 rpm for 30 min. The aqueous phase was removed and frozen until analyzed for the U.S. Environmental Protection Agency (U.S. EPA) SW-846 analytes plus 2,6-DANT, 2,4-DANT, and 4,4-Azoxo. The aqueous samples from the Yokena clay were preserved with ethylene-diamine-tetraacetic acid to a final concentration of 5 μM . The testing was carried out in duplicate for each soil examined. Table 3 lists the measured soil–water partition coefficients (K_{sw}) values for the three compounds with the three different soils.

Analytical methods

Soils in the flux chambers were analyzed initially and at the end of each experiment to determine if explosive degradation occurred during the experiment. Air sampling traps were extracted for 24 h with acetonitrile before analysis. At the conclusion of an experiment, the plate at the top of the flux apparatus was rinsed with acetonitrile to determine if any residues remained on the chamber surface. Analyses of soils, sampling trap acetonitrile extracts, and acetonitrile rinses of flux chamber surfaces were performed using U.S. EPA SW-846 Method 8330 [7].

RESULTS AND DISCUSSION

Theory and model

The most general model describing contaminant fate and transport in porous media is a diffusion–reaction equation with a diffusive boundary condition at the surface and a semi-infinite boundary condition at the bottom. Diffusion in the soil pore air is assumed to be the dominant mechanism of mass transport within the soil. The reaction term is added for generality to accommodate disappearance due to biodegradation or reaction within the soil. The model also neglects wicking as a possible mechanism for vapor phase contaminant transport. Equation 1 is the governing differential equation for the pore air concentration of the contaminant, $C_A(z, t)$ as a function of depth (z) and time (t):

$$\frac{\partial C_A}{\partial t} = \frac{D_{\text{eff}}}{R_f} \frac{\partial^2 C_A}{\partial z^2} - k_1 C_A \quad (1)$$

with boundary conditions at $z = 0$ (surface)

$$k_a C_A = D_{\text{eff}} \frac{\partial C_A}{\partial z} \quad (2)$$

and at $z = \infty$, $C_A = C_A^0$.

The analytical solution [8] to Equation 1 gives $C_A(z, t)$. The flux is calculated by multiplying the surface overall mass transfer coefficient, k_a , and the vapor phase contaminant concentration at the surface, $C_A(0, t)$ and the resultant expression for flux $N_A(t)$ is shown in Equation 2.

$$N_A(t) = C_A^0 k_a e^{-k_1 t} \exp\left(\frac{k_a^2 t}{D_{\text{eff}} R_f}\right) \text{erfc}\left(k_a \sqrt{\frac{t}{D_{\text{eff}} R_f}}\right) \quad (3)$$

In Equation 3, C_A^0 is the initial equilibrium concentration of the contaminant in the pore air and is given by $W_S^0 \rho_b / R_f$, where W_S^0 was the initial loading of the contaminant (kg/kg), ρ_b is the bulk density of the soil (kg/m³), and R_f is the retardation factor. The air-side mass transfer coefficient is denoted by k_a , D_{eff} is the effective diffusivity of a chemical A in the soil pore air, and k_1 is a first-order rate constant for disappearance of chemical in soil.

The model described by Equation 1 assumes local equilibrium with respect to the contaminant in the pore spaces. Further, the surface flux depends on the soil-side and air-side resistances offered to transport of the contaminant [3]. The soil-side resistance is dependent on the retardation of the contaminant on the soil surface due to adsorption and the effective diffusivity of the contaminant in the porous media. The retardation factor is given by $\epsilon_a + \rho_b K_{SA}$, where K_{SA} is the soil–air partition constant (L/kg). The retardation factor is proportional to the partition constant of the contaminant between soil and air (K_{SA}). In the absence of direct measurements, K_{SA} can be estimated for wet soils (>5% soil moisture content) using Equation 4:

$$K_{SA} = \frac{K_{sw}}{K_{AW}} \quad (4)$$

where K_{sw} is the soil–water partition constant (L/kg) and K_{AW} is the air–water partition constant (Henry's law constant, molar concentration ratio, dimensionless). The soil–water partition constants (K_{sw}) were directly measured for the compounds of interest in separate batch experiments. In the absence of measured data, the values of the Henry's constant for the compounds of interest were obtained from the ratio of the saturated vapor pressure and solubility of UXOs in water. The uncertainty in the Henry's constant values directly translates to the uncertainty in the soil–air partition constant.

The effective diffusivity, D_{eff} , was computed using the expression $D_A \epsilon_a^{10/3} / \epsilon_T^2$, where ϵ_a is the air-filled porosity and ϵ_T is the total porosity [8]. The values of air-filled porosity used in the simulation were calculated using the measured values of the initial soil moisture content, total soil porosity, and soil bulk density. The mass transfer coefficient, k_a , quantifies the air-side resistance offered by the film for mass transfer between the soil surface and the air flowing over the surface. It was estimated using the boundary layer theory, $0.664 \text{Re}^{0.33} \text{Sc}^{0.5} (D_A/d)$, where Re is the Reynolds number, Sc is the Schmidt number, D_A is the diffusivity of the chemical A in air, and d is the length of the airflow path. The term Re is given by $d \cdot v / \nu$, where ν is the average flow velocity, ν is

the kinematic viscosity of air, and Sc is given by ν/D_A . The reaction rate constant k_1 was set to zero in all simulations. All parameters were assumed to be constant during the simulation.

Wicking can be an important transport mechanism when continuous replenishment of soil moisture occurs from beneath the top layers of soil during surface drying. The laboratory experiments described in this manuscript were performed with a very thin layer of soil (2 cm) that had a low moisture content (5 and 20%) and no water replenishment from below.

The losses from any possible wicking can be estimated by $k_{adv} \cdot C_{air}^0$, where k_{adv} is the advective velocity that may be induced by wicking and C_{air}^0 is the equilibrium vapor phase concentration of the chemical in the soil. The advective velocity of pore air saturated with water vapor was calculated from a previous study [5] and corrected for the difference in airflow rates used in both studies based on soil to air mass transfer coefficients in the literature [9] and was found to be $0.034 \text{ cm}^3/\text{cm}^2/\text{h}$. The advective fluxes thus computed for the three chemicals in cases 1 and 3 shown in this manuscript range from 7.4×10^{-6} to $0.025 \text{ ng}/\text{cm}^2/\text{h}$. The experimental fluxes measured at times below 72 h (time period when steady state water evaporation is expected to occur) range from 0.0083 to $17.2 \text{ ng}/\text{cm}^2/\text{h}$. The ratios of the computed advective fluxes to the corresponding measured experimental fluxes range from 0.00044 to 0.05. In the worst case, the advective fluxes are 5% of the measured fluxes. This analysis shows that for chemicals that exhibit very low vapor pressures and very high partition constants, wicking was not a significant mechanism for vapor phase transport and was therefore neglected in the transport model described in this manuscript.

Experimental soil–water adsorption constants

The aquifer soils from LAAP were higher in sand, ranging from 27 to 77% sand and low in organic carbon (Table 1). Silt and clay were present in all samples, although in lower amounts. Cation exchange capacity (CEC) was also relatively low, ranging from 6.6 to 15.5 meq/100 g. This is in marked contrast to the Yokena clay surface soil that was high in clay, organic carbon, and CEC (Table 1) compared to the aquifer soils.

The experimentally measured soil–water partition constants (K_{SW}) for 2,4-DNT, 2,6-DNT, and 1,3-DNB are listed in Table 3. The K_{SW} values for the Yokena clay surface soil were found to be larger than those for the aquifer soils. Previous work on a UXO (2,4,6-trinitrotoluene) showed that the K_{SW} for nitrocompounds was strongly correlated to the CEC and clay content of the soil [10,11]. In the present work, we realized a similar trend. The K_{SW} for all four compounds increased with CEC, clay content, and organic carbon fraction of the soils. It is clear that sorption of these compounds is higher in the surface soil (Yokena clay) than in aquifer soils (LAAP-C and LAAP-D).

Experimental data and model simulations

Experimental data analyzed using the model was classified under three cases on the basis of the experimental conditions (initial soil moisture content and relative humidity of air passing over soil surface).

Case 1. The initial moisture content of the soil was 5%, and the relative humidity of the air passing over the soil surface was 100%. The soil pore air was water saturated and hence was expected to retain the initial moisture content since no moisture loss is expected. The initial air-filled porosity was

Table 4. Sediment properties for simulation

Experiment	Initial soil moisture	Air relative humidity	Air-filled porosity (ϵ_a)	Water-filled porosity (ϵ_w)	Total porosity (ϵ_T)
Case 1	5%	Humid	0.08	0.23	0.31
Case 2	20%	Dry	0.16	0.15	0.31
Case 3	5%	Dry	0.31	0	0.31

calculated to be 0.08 and was maintained at that value throughout the simulation period. With humid air passing over the surface, the soil was considered to be wet at that soil moisture content, and therefore the K_{SA} was estimated from K_{SW} and K_{AW} as per Equation 4.

Case 2. The initial moisture content of the soil was 20%, and the relative humidity of the air passing over the soil surface was 0%. The soil moisture filled almost all the soil pores initially, but with moisture loss to air, the air-filled porosity was expected to increase. Earlier reports of water evaporation rates from similar experiments [5] showed that initially water loss occurs very rapidly and that complete water loss takes much longer. The air-filled porosity would increase as a function of time during this period, but in the absence of any transient measured data, the air-filled porosity was set as an average of the initial (zero) and the final expected value (total porosity). For the duration of the experiment, the soil was presumed to retain enough moisture to be considered wet, and the K_{SA} was estimated from K_{SW} and K_{AW} as per Equation 4.

Case 3. The initial moisture content of the soil was 5%, and the relative humidity of the air passing over the soil surface was 0%. The moisture from the pore-air space was expected to decrease within a very short period of time, and therefore the value of the air-filled porosity was set equal to that of the total porosity throughout the simulation period. The rapid drying creates the possibility of dry-off of the soil surface. In this case, K_{SA} cannot be approximated as K_{SW}/H_C and was not directly measured either. As an adjustable parameter, K_{SA} was used in the model for this case. The porosity values used in each case of the simulation are summarized in Table 4.

Figures 1 to 3 show the comparison of experimental fluxes and the corresponding model simulations for 2,4-DNT, 2,6-DNT, and 1,3-DNB, respectively, at 24°C from three different soils for cases 1 and 2. These three compounds were chosen for comparison since the data set was most complete for these. Figure 1a, b, and c shows the flux of 2,4-DNT from LAAP-C, LAAP-D, and Yokena soils, respectively. The experimental flux values are represented by discrete symbols, while the simulation curves are represented by lines. The experimental data show the flux of 2,4-DNT decreasing gradually with time and quickly reaching a steady state. Initially, the flux is air-phase-resistance controlled. Very quickly, it becomes soil-side-resistance controlled, and diffusion through the soil pores dominates. Thus, the initial flux can be given by $N_A(t) = k_a C_A^0$, and as t becomes large, the long-term flux is given by $N_A = C_A^0 \sqrt{(R_f D_{eff} / \pi t)}$. The diffusion-controlled flux is proportional to $1/t^{1/2}$. Any deviation from this behavior is indicative of processes other than diffusion also being significant. Figures 2 and 3 show similar trends in the experimental fluxes of 2,6-DNT and 1,3-DNB, respectively, for cases 1 and 2 for the three soils.

The model curves in each case shown in Figures 1 to 3 were not a priori simulations but best fits of the experimental

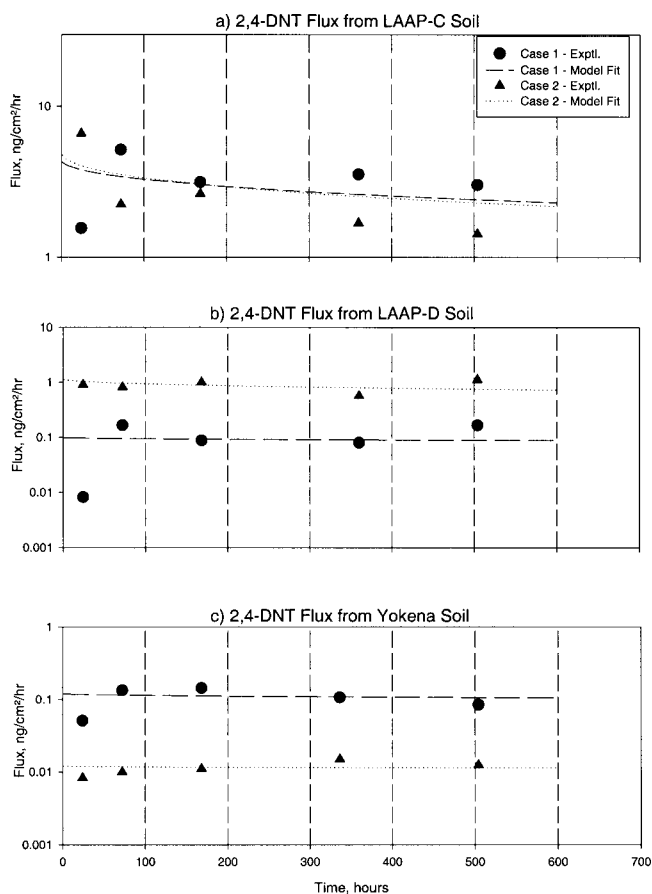


Fig. 1. Flux of 2,4-dinitrotoluene (DNT) from three soils. Comparison of experimental data and model fits for cases 1 and 2.

data using a one-variable fit parameter—the soil–air partition constant, K_{SA} . The best fit for each data set was obtained by adjusting the K_{SA} value until the sum of squares quantity between the experimental data and model fit was a minimum. The model fit curves show a trend similar to that of the experimental data. The effectiveness of the model to simulate the experimental fluxes can be evaluated by comparing the experimentally determined and fit model parameters, in this case, K_{SA} . Table 5 shows this comparison of the K_{SA} values for cases 1 and 2 for the three compounds and the three soil types. The average difference between the fit and the a priori estimation of K_{SA} is within an order of magnitude for all compounds. The K_{SW} values used to estimate K_{SA} were those measured in the batch experiments, and hence the variation in K_{SA} is directly a result of the variation in reported K_{AW} (Henry's constant) values.

Figure 4 shows the experimental data for case 3. The experimental data show a distinct sharp downward gradient with time not characteristic of a $1/t^{1/2}$ dependence for purely diffusive transport as observed in the cases 1 and 2. This behavior is uniformly observed for all three compounds and for the three soil types as seen in Figure 4. This trend is not indicative of an equilibrium state in the soil as seen in Figures 1 to 3. It is more representative of a dynamic rate-controlled (kinetic) phenomenon. Two hypotheses arise out of these observations.

First, the soil is drying at a very small rate, and the initial moisture content was at the edge of the wet soil criteria (5% moisture content) for soil–air partition constants described earlier. The soil partition constant increases as soil moisture de-

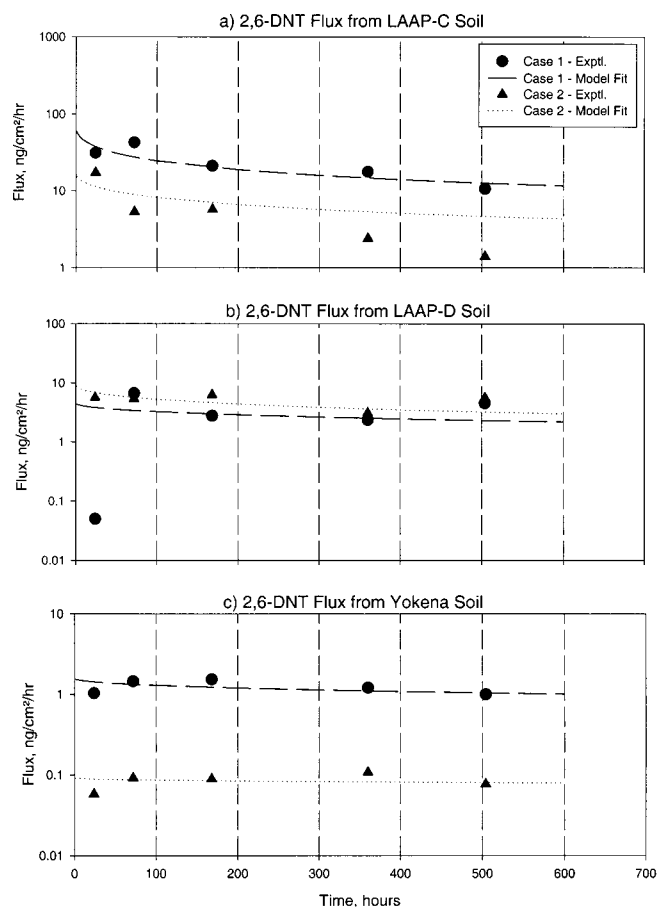


Fig. 2. Flux of 2,6-dinitrotoluene (DNT) from three soils. Comparison of experimental data and model fits for cases 1 and 2.

creases below 5% and continues to decrease until the soil moisture level reaches the dry state and is constant for soil moisture levels below 0.1%. The rate of decrease of the partition constant in the damp zone between the dry and the wet zone is not well characterized and depends on the drying rate of the soil, which is dependent on the flow rate of air and initial moisture content. Therefore, decreasing flux measurements might represent successive stages of increasing partition constant, as the soil is still undergoing loss of moisture in the damp regime due to the low moisture content and the low airflow rate (20 ml/min). The experiment was concluded before the flux measurements attained a plateau indicative of an equilibrium state (completion of the drying process), when an equilibrium partition constant of the dry soil could have been extracted by fitting the dry flux data. Experiments performed at higher airflow rates can provide more qualitative information for the UXO soil–air partitioning in the dry soils in the time scales of the experiments performed.

A second hypothesis is that the soil is dry enough to cause a surface reaction to degrade the UXO compound. Such a loss via reaction can be coupled with a purely diffusive transport to model the transport process. The gradient in the flux data observed may be representative of the surface reaction kinetics on dry soils. Since no batch experiments were performed to evaluate the reaction kinetics on dry soil, it is not possible to verify or evaluate this hypothesis at this stage. It can only be surmised that the system is tending toward a new equilibrium state not captured in the time scale of the experiment. Previous references exist of oligomerization reactions on dry mineral

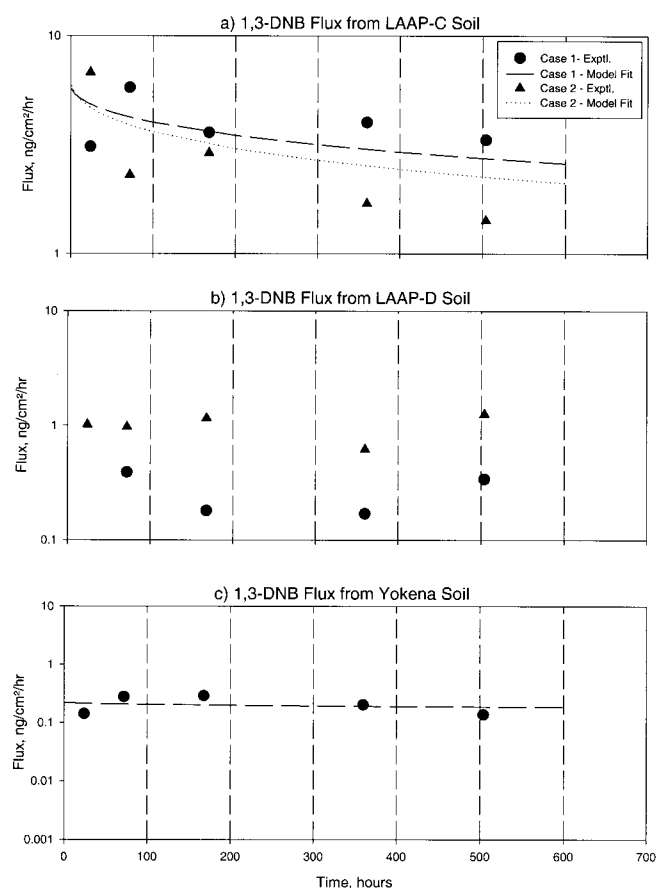


Fig. 3. Flux of 1,3-dinitrobenzene (DNB) from three soils. Comparison of experimental data and model fits for cases 1 and 2.

surfaces of soils with very low organic carbon. This phenomenon has been observed by Karimi-Loftabad et al. [12] for polyaromatic hydrocarbons on dry soils. It would be informative to measure the disappearance rates and the adsorption half-lives of explosive compounds, used in this study, on dry soils in separate batch studies to determine the validity of this hypothesis.

Effect of soil temperature on flux from soils

Since temperature is an important variable among the various DOD sites contaminated with explosives residues, we conducted one set of experiments to elucidate the effect of soil

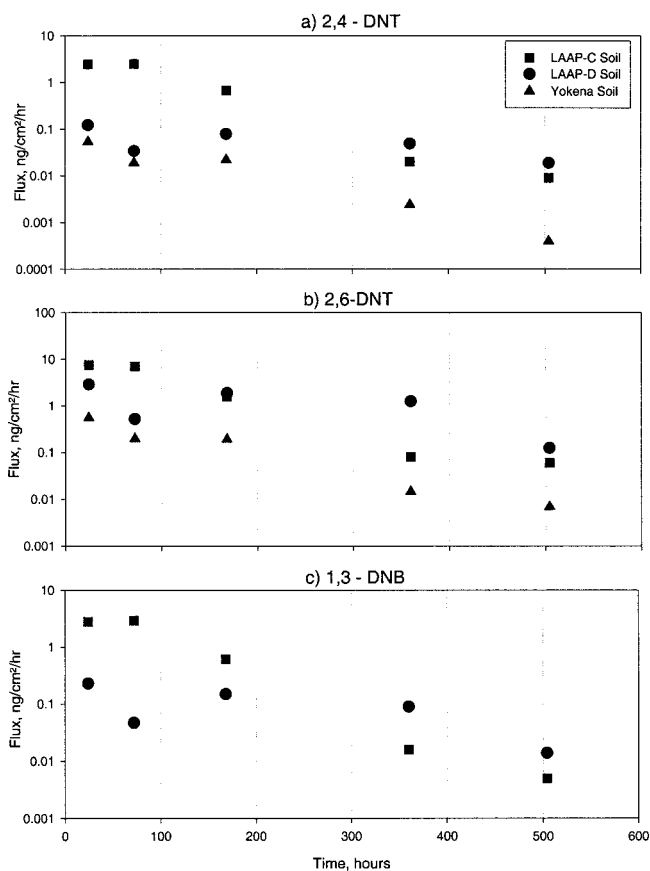


Fig. 4. Experimental fluxes for case 3 for 2,4-dinitrotoluene (DNT), 2,6-DNT, and 1,3-dinitrobenzene (DNB) from three soils for cases 1 and 2.

temperature on flux to air. Figure 5 shows the comparison of 2,4-DNT flux from LAAP-C soil samples at two different temperatures: 14 and 24°C (room temperature) for case 2. The flux was 0.51 ng/cm²/h at 14°C and 6.63 ng/cm²/h at 24°C after 24 h and slowly decreased to 0.11 ng/cm²/h at 14°C and 1.43 ng/cm²/h at 24°C after 504 h. The flux at 14°C was uniformly lower than that at 24°C. Figure 5 also shows the model fit curves for the experimental data for both temperatures. The model simulation for the 24°C case was described earlier in this section. The model fit to the data at 14°C was performed with the K_{SA} obtained at 24°C as a starting value. A correct fit was obtained by changing K_{SA} and minimizing the residual

Table 5. Adjustable parameter for comparison with experimental flux from case 1 and case 2^a

	LAAP-C		LAAP-D		Yokena clay	
	Case 1	Case 2	Case 1	Case 2	Case 1	Case 2
2,4-DNT						
K_{SA} (L/kg) (estimated)	8.9e + 4	8.9e + 4	2.2e + 5	2.2e + 5	1.7e + 6	1.7e + 6
K_{SA} (L/kg) (fit)	1.2e + 5	1.1e + 5	5.5e + 6	4.8e + 5	4.2e + 6	4.2e + 7
2,6-DNT						
K_{SA} (L/kg) (estimated)	1.3e + 5	1.3e + 5	2.4e + 5	2.4e + 5	7.9e + 5	7.9e + 5
K_{SA} (L/kg) (fit)	6.4e + 3	2.5e + 4	9.6e + 4	4.7e + 4	3.2e + 5	5.5e + 6
1,3-DNB						
K_{SA} (L/kg) (estimated)	9.9e + 3	9.9e + 3	NA ^b	NA	5.5e + 5	5.5e + 5
K_{SA} (L/kg) (fit)	6.1e + 4	6.9e + 4	NP ^c	NP	2.3e + 6	ND ^d

^a Refer to Table 1 for definitions of abbreviations.

^b NA = experimental K_{SW} not available and hence K_{SA} not estimated.

^c NP = no model fit performed since K_{SW} measurement was not available.

^d ND = no experimental data.

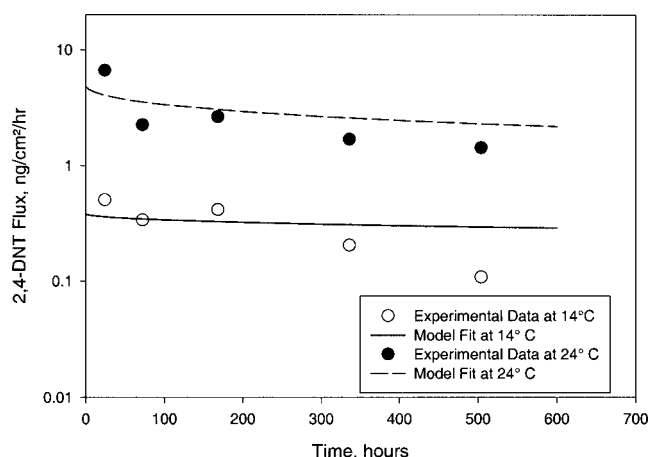


Fig. 5. Effect of temperature on the flux of 2,4-dinitrotoluene (DNT) from LAAP-C soil (case 2: 20% moisture content with dry air passing over the soil; soil obtained from Louisiana Army Ammunition Plant, Shreveport, LA, USA).

sum of square of errors. A correction factor of $(T_2/T_1)^{7/4}$ was used to adjust the diffusivity to the lower temperature [9]. The fit K_{SA} for 2,4-DNT on LAAP-C soil at 14°C was 10^7 L/kg as compared to 1.2×10^5 L/kg at 24°C. Since the soil–water partition constant was not experimentally measured at 14°C, it was not possible to evaluate the degree of deviation from the expected K_{SA} estimation using Equation 4. However, the trend of higher partitioning constant at lower temperature was compared to the data obtained for a different compound (phenanthrene) on a different soil but with comparable moisture contents. The heat of desorption from soil to air, ΔH_{desorp} , was calculated using the Clausius–Clapeyron equation:

$$\frac{d(\ln P)}{dT} = -\frac{\Delta H_{desorp}}{RT^2} \quad (5)$$

where P is the equilibrium vapor pressure (Pa) calculated using Equation 6,

$$P = \frac{W_s RT}{K_{SA} M} \quad (6)$$

where W_s is contaminant loading (kg/kg), M is the molecular mass, and K_{SA} is the soil–air partition constant (m^3/kg). ΔH_{desorp} of 187 kJ/mol was obtained from Equation 5 and indicated that desorption was endothermic. The heat of desorption for phenanthrene measured by Deseze [13] was also endothermic (average value of ΔH_{desorp} for wet soil was 90 ± 4 kJ/mol). This suggests that the effect of temperature on K_{SA} and flux for UXO are similar to those reported for other types of compounds and are predictable using Equation 3 with appropriate temperature correction for K_{SA} .

CONCLUSIONS

The predicted volatilization rates were dependent on the measurement and estimation of the soil–air partition constant, K_{SA} . In general, in all cases a slowly decreasing flux seemed to exist, which is in agreement with the trend in the model fit curves. The average variation of the fit partition constants were within an order of magnitude and is realistic considering the wide variation in measured or estimated Henry's constant values reported in the literature. The sharp decrease in flux shown by the experimental data involving dry soil suggests increasing

partition constants due to the dynamics of drying or surface reaction with first-order kinetics. The mechanism governing this rapid decrease should be further studied in separate batch experiments. The observed fluxes at 14°C were lower than that obtained at 24°C. This is due to the expected lower partition constants at lower temperature. The partitioning of explosive compounds to the soils at lower temperatures have to be measured in order to derive a correlation to estimate the partition constants. This will facilitate the prediction of volatile flux rates from various UXO sources at different temperatures. Further experiments should also be conducted to measure the volatile UXO fluxes through a layer of clean cap material on top of the contaminated soil sample to simulate the conditions in the field where the UXOs are buried under layers of soil.

Acknowledgement—This study was supported by the U.S. Army Engineering Research and Development Center (Vicksburg, MS, USA) through the U.S. Army Corps of Engineers Installation Restoration Research Program (Grant DACW42-00-P-0113).

REFERENCES

1. U.S. Department of Defense. 1992. Defense environmental restoration program: Annual report to Congress for fiscal year 1991. Government Printing Office, Washington, DC.
2. McGrath CJ. 1995. Review of formulations for processes affecting the subsurface transport of explosives. IRRP-95-2. Technical Report. U.S. Army Engineer Corps of Engineers Waterways Experiment Station, Vicksburg, MS.
3. Valsaraj KT, Ravikrishna R, Choy B, Reible DD, Thibodeaux LJ, Price CB, Brannon JM, Myers TE. 1999. Air emissions from exposed, contaminated sediments and dredged materials. *Environ Sci Technol* 32:142–149.
4. Ravikrishna R, Valsaraj KT, Yost S, Price CB, Brannon JM. 1997. Air emissions from exposed, contaminated sediments and dredged materials 2. Diffusion from laboratory-spiked and aged field sediments. *J Hazard Mater* 60:89–104.
5. Valsaraj KT, Ravikrishna R, Choy B, Reible DD, Thibodeaux LJ, Price CB, Brannon JM, Myers TE. 1997. Air emissions from exposed, contaminated sediments and dredged materials 1. Experimental data in laboratory microcosms and mathematical modeling. *J Hazard Mater* 54:65–87.
6. Spencer WF, Shoup TD, Cliath MM, Farmer WJ, Haque R. 1979. Vapor pressure and relative humidity of ethyl and methyl parathion. *J Agric Food Chem* 27:273–278.
7. U.S. Environmental Protection Agency. 1990. High performance chromatographic methods for analysis of nitroaromatics and nitroamines. Method 8330. In *Test Methods for Evaluating Solid Waste—Physical and Chemical Methods—SW-846*, Vol 1B, 2nd ed. National Technical Information Services, Springfield, VA.
8. Choy B, Reible DD. 2000. *Diffusion Models of Environmental Transport*. Lewis, Boca Raton, FL, USA.
9. Thibodeaux LJ. 1996. *Environmental Chemodynamics*. Wiley Interscience, New York, NY, USA.
10. Pennington JC, Patrick WH Jr. 1990. Adsorption and desorption of 2,4,6-trinitrotoluene by soils. *J Environ Qual* 19:559–567.
11. Haderlein SB, Weissmahr KW, Schwarzenbach RP. 1996. Specific adsorption of nitroaromatic explosives and pesticides to clay minerals. *Environ Sci Technol* 30:612–622.
12. Karimi-Loftabad S, Pickard MA, Gray MR. 1996. Reaction of polynuclear aromatic hydrocarbons on soils. *Environ Sci Technol* 30:1145–1151.
13. DeSeze G. 2000. Sediment-air partitioning of hydrophobic organic chemicals. PhD thesis. Louisiana State University, Baton Rouge, LA, USA.
14. Pennington JC, Gunnison D, Harrelson DW, Brannon JM, Zakikhani M, Jenkins TF, Clarke JM, Hayes CA, Myers TE, Perkins E, Ringelberg D, Townsend DM, Fredrickson H, May JH. 1999. Natural attenuation of explosives in soil and water systems at Department of Defense sites. EL-99-8. Interim Technical Report. U.S. Army Corps of Engineers Waterways Experiment Station, Vicksburg, MS.